SOLVING POWER-CONSTRAINED GAS TRANSPORTATION PROBLEMS USING AN MIP-BASED ALTERNATING DIRECTION METHOD

BJÖRN GEISSLER[1], ANTONIO MORSI[1], LARS SCHEWE[1], MARTIN SCHMIDT[2]

Abstract. We present a solution algorithm for problems from steady-state gas transport optimization. Due to nonlinear and nonconvex physics and engineering models as well as discrete controllability of active network devices, these problems lead to hard nonconvex mixed-integer nonlinear optimization models. The proposed method is based on mixed-integer linear techniques using piecewise linear relaxations of the nonlinearities and a tailored alternating direction method. In addition to most other publications in the field of gas transport optimization, we do not only consider pressure and flow as main physical quantities but further incorporate heat power supplies and demands as well as a mixing model for different gas qualities. We demonstrate the capabilities of our method on Germany's largest transport networks and hereby present numerical results on the largest instances that were ever reported in the literature for this problem class.

The optimization of real-world gas transport networks is a mathematically challenging task. The combination of highly nonlinear and nonconvex models of gas dynamics and engineering together with the discrete nature of controllable network devices leads to large-scale nonconvex mixed-integer nonlinear optimization or feasibility problems (MINLPs). The size of the networks result in instances that are far beyond of being solvable by general-purpose MINLP solvers and thus call for tailored optimization methods.

The main contribution of this article is a tailored alternating direction method (ADM) that is based on mixed-integer linear (MIP) models. This combination enables us to solve MINLP problems on gas transport networks of sizes that were never reported before in the literature. Furthermore, we extend standard models of gas transport such that mixing of different gas qualities is also considered. In this way, we can satisfy heat power constraints that are of crucial importance in practice. The standard setting of gas network optimization is to prescribe bounds on the pressure and the mass flow at supply and demand nodes. Using mass flow is the natural setting from the physical point of view as mass flow is a conserved quantity. From the point of view of a network planner, however, the more natural quantity is heat power as it is the quantity that is used in contracts with the customers. Heat power is simply the product of mass flow and the calorific value of the gas. At supply nodes, the calorific value is given so that there is no distinction between these two notions. For demand nodes, however, the calorific value depends on the mixture of the gas, which is highly dependent on the specific flow situation and thus cannot be computed a priori. The gas quality of different sources in typical European networks vary such that the effects of mixing are substantial. Thus, for the practical application of automated methods in network planning it is important

Date: November 27, 2014.

2010 *Mathematics Subject Classification.* 65K10, 90-08, 90B10, 90C06, 90C11, 90C35, 90C90.

Key words and phrases. Nonconvex Mixed-Integer Nonlinear Optimization, Alternating Direction Methods, Piecewise Linear Relaxations, Gas Transport Networks, Heat Power Supply and Demand.

to adequately model these effects. The main challenge is that one has to deal with the additional complexity of a pooling problem on top of the high complexity of the gas network optimization problem. The resulting MINLP is by far too difficult to be tackled with off-the-shelf MINLP solvers. There are two typical approaches to derive algorithms to construct feasible solutions for specific MINLPs: One approach is to use classical methods of nonlinear optimization, specifically local methods, and try to reformulate the model such that the discrete variables can be removed, e.g., by introducing complementarity constraints [31]. The other approach, which we use in this article, is to approximate and/or relax nonlinear constraints using piecewise linear functions. We use a technique that is first discussed in [13] to construct MIP relaxations for flow-based models; see also [12, 18]. By combining these MIP relaxations for flow-based models with an alternating direction method, we are able to find feasible solutions for large-scale real-world instances of heat power constrained gas transport problems.

The question how to adequately treat heat power in transport models has already been discussed in the literature. Typically, the additional complexity of considering heat power makes it necessary to simplify the physics of gas transport. For instance, Tomasgard et al. [34] simplify the pressure drop equation by using a coarse linearization. In Li et al. [20] the pressure drop is completely neglected. Van der Hoeven [36] also discusses gas quality and mixing but uses simplifications leading to linear approximations of mixing models. For a general overview of the gas network optimization literature we refer to [18, Chapter 5].

The paper is organized as follows: In Section 1, we introduce the (stationary) problem under consideration and present a mixed-integer nonlinear feasibility model. The techniques for obtaining linear relaxations of the MINLP are briefly sketched in Section 2. Afterward, we reformulate the MINLP in order to apply a tailored ADM in Section 3, where the main convergence properties of ADMs are also reviewed. Due to nonconvexity and nonsmoothness of the considered problem, the convergence results are rather weak. To improve the quality of solutions achieved by the ADM, we heuristically modify the method and present our numerical results on large-scale real-world networks in Section 4. Finally, the paper closes with a brief summary and an outlook in Section 5.

1. The Problem

Our problem is to find values of the controls and states of a gas network such that all physical, technical, and heat power constraints are satisfied. The model we use is a variant of the model discussed in [18, Chapter 6]. The main extension is the introduction of heat power variables and the respective constraints.

In this section, we present the model of the network (Section 1.1) and models for all of its elements; see Section 1.2–Section 1.3. In Section 1.4, we discuss so-called subnetwork operation modes and in Section 1.5, we present the heat power and mixing model. We close with a summary and a brief discussion of the model in Section 1.6.

Readers interested in more details concerning gas network or fluid flow modeling are referred to [21, 30] in general or to [18] for the underlying models presented here in particular.

1.1. Network Model and Basic Physical Quantities.

We model a gas network as a directed graph $G = (V, A)$ with node set V and arc set A. The set of nodes is partitioned into the set of entry nodes V_+, at which gas is supplied, the set of exit nodes V_-, where gas is withdrawn, and the set of inner nodes V_0. The arcs consist of pipes A_{pi}, resistors A_{rs}, valves A_{va}, control valves A_{cv}, and compressor machines A_{cm}.

Gas flow in networks is mainly described by mass flow q, heat power P, and the three gas state quantities pressure p, temperature T, and density ρ. The state quantities are coupled by an equation of state. Here we use the thermodynamical standard equation for real gases

$$\rho R_{\mathrm{s}} z T = p,$$

where R_{s} is the specific gas constant and z is the compressibility factor that we model using the formula of Papay [25]:

$$z(p,T) = 1 - 3.52 p/p_{\mathrm{c}} e^{-2.26T/T_{\mathrm{c}}} + 0.247 (p/p_{\mathrm{c}})^2 e^{-1.878T/T_{\mathrm{c}}}. \tag{1}$$

The quantities p_{c} and T_{c} are the pseudocritical pressure and temperature, respectively, which we assume to be constants. Throughout the paper, we assume isothermal gas flow, i.e., we fix the gas temperature at a suitable constant value. We associate positive gas flow on arcs $a = (u,v)$ with flow in arc direction, i.e., $q_a > 0$ if gas flows from u to v and $q_a < 0$ if gas flows from v to u. The sets $\delta^{\mathrm{in}}(u) := \{a \in A : a = (v,u)\}$ and $\delta^{\mathrm{out}}(u) := \{a \in A : a = (u,v)\}$ are the sets of in- and outgoing arcs and the sets

$$\mathcal{I}(u) := \{a \in \delta^{\mathrm{in}}(u) : q_a \geq 0\} \cup \{a \in \delta^{\mathrm{out}}(u) : q_a \leq 0\},$$
$$\mathcal{O}(u) := \{a \in \delta^{\mathrm{in}}(u) : q_a < 0\} \cup \{a \in \delta^{\mathrm{out}}(u) : q_a > 0\}$$

are the sets of in- and outflow arcs of node u.

1.2. **Nodes.** For each node $u \in V$, we assume lower and upper values p_u^- and p_u^+ to be given that bound the corresponding pressure variable p_u, i.e.,

$$p_u \in [p_u^-, p_u^+] \quad \text{for all } u \in V. \tag{2}$$

In addition, we model mass conservation at each node of the network by Kirchhoff's first law, i.e.,

$$\sum_{a \in \delta^{\mathrm{out}}(u)} q_a - \sum_{a \in \delta^{\mathrm{in}}(u)} q_a = q_u \quad \text{for all } u \in V, \tag{3}$$

where $q_u \geq 0$ for entries, $q_u \leq 0$ for exits, and $q_u = 0$ for inner nodes.

1.3. **Arcs.** For every arc $a \in A$ there is a mass flow variable q_a that is bounded from below and above, i.e.,

$$q_a \in [q_a^-, q_a^+] \quad \text{for all } a \in A. \tag{4}$$

We now present the models of all arc types, starting with pipes.

1.3.1. *Pipes.* A pipe $a \in A_{\mathrm{pi}}$ is used to transport the gas through the network. Pipes outnumber all other network elements. A pipe is specified by its length L_a, its diameter D_a and its integral roughness k_a. We assume each pipe to be cylindrically shaped and to have a constant slope s_a. In this situation, gas flow through a pipe is described by a system of partial differential equations—the Euler equations for compressible fluids [6]—consisting of the continuity and the momentum equation. In a stationary regime, the former reduces to constant mass flow along a pipe. The momentum equation describes the pressure loss due to ram pressure, frictional forces, and gravity. We make the additionally simplifying assumptions that the compressibility factor z can be approximated by a constant mean value and that the ram pressure term of the momentum equation can be neglected; see [38]. Then the model of pressure loss along a pipe is given by

$$p_v^2 - c_{1,a} p_u^2 = c_{2,a} \, |q_a| \, q_a \quad \text{for all } a = (u,v) \in A_{\mathrm{pi}}, \tag{5}$$

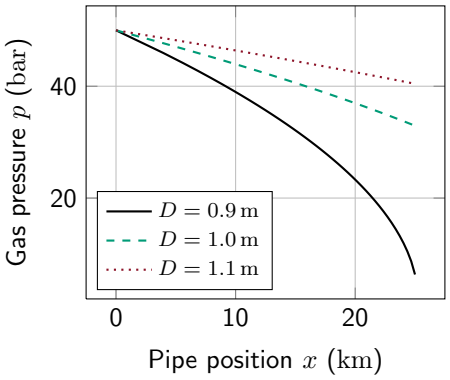

FIGURE 1. Pressure profiles of three horizontal pipes with $L = 25\,\mathrm{km}, k = 0.06\,\mathrm{mm}, q = 500\,\mathrm{kg\,s^{-1}}$ and different diameters; see [18].

with nonnegative constants

$$c_{1,a} = e^{-S_a}, \quad c_{2,a} = \begin{cases} -\Lambda_a (e^{S_a} - 1)/S_a e^{-S_a} & \text{if } s_a \neq 0, \\ -\Lambda_a, & \text{otherwise,} \end{cases}$$

and

$$\Lambda_a = \frac{L_a \lambda_a R_\mathrm{s} z_\mathrm{m} T}{A_a^2 D_a}, \quad S_a = 2g \frac{s_a L_a}{R_\mathrm{s} z_\mathrm{m} T}, \quad z_\mathrm{m} = z(p_{\mathrm{m},a}, T).$$

Here, λ_a is the friction coefficient (modeled by Nikuradse's formula [23]), g is the gravitational acceleration, and z_m is the mean compressibility factor. The latter is computed by using the mean pressure along the pipe:

$$p_{\mathrm{m},a} = \frac{1}{2} \left(\max \left\{ p_u^-, p_v^- \right\} + \min \left\{ p_u^+, p_v^+ \right\} \right).$$

The cross-sectional area of the pipe is given by $A_a = D_a^2 \pi / 4$. The reader interested in the deviation of this model and other (more detailed) models is referred to [18, 33, 32] and the references therein. Typical profiles of pressure loss in a pipe are given in Figure 1.

We finally remark that we also consider so-called *short pipes* that are used as auxiliary network elements with negligible pressure loss; see [18] for the details. These short pipes $a = (u, v)$ are simply modeled by equal in- and outflow pressure, i.e., $p_u = p_v$.

1.3.2. *Resistors.* A resistor $a \in A_\mathrm{rs}$ is used to model pressure losses that are caused by filter or measurement devices, station piping, etc. We distinguish two different types of resistors: resistors with constant pressure loss ($A_{\text{lin-rs}}$) and resistors with a nonlinear pressure loss ($A_{\text{nl-rs}}$). Thus, $A_\mathrm{rs} = A_{\text{lin-rs}} \cup A_{\text{nl-rs}}$. Both types induce a pressure drop in flow direction. A resistor with a nonlinear (Darcy–Weisbach type; see [7]) pressure loss is modeled by

$$p_u^2 - p_v^2 + |\Delta_a| \, \Delta_a = 2 c_a \, |q_a| \, q_a, \quad \Delta_a = p_u - p_v, \tag{6}$$

with $c_a = 8 \zeta_a R_\mathrm{s} T_\mathrm{m} z_{\mathrm{m},a} / (\pi^2 D_a^4)$, where $\zeta_a > 0$ is the so-called drag factor.

A resistor $a = (u, v) \in A_{\text{lin-rs}}$ is specified by a fixed pressure drop ξ_a and the pressure values at nodes u and v are related by

$$p_u - p_v = \operatorname{sgn}(q_a) \xi_a \approx \begin{cases} \xi_a & \text{if } q_a \geq \varepsilon, \\ -\xi_a & \text{if } q_a \leq -\varepsilon, \\ \xi_a / \varepsilon q_a, & \text{otherwise.} \end{cases} \tag{7}$$

The deviation of these models and a specific MINLP formulation can again be found in [18].

1.3.3. *Valves.* A valve $a \in A_{\text{va}}$ is a network element of purely combinatoric nature. Valves can be *open* or *closed*. If open, gas can flow through the valve and in- and outflow pressures are equal, i.e., $p_u = p_v$. If closed, the valve restricts the gas from passing, i.e., $q_a = 0$. Hence, the model reads

$$a \text{ is open} \implies p_u = p_v, \tag{8a}$$

$$a \text{ is closed} \implies q_a = 0. \tag{8b}$$

1.3.4. *Control Valves.* A control valve $a \in A_{\text{cv}}$ is used to decrease pressure. This is mainly required at transition points between large transport pipelines and regional substructures that are not able to handle high pressures. There exist two different types of control valves; those that are remotely controllable and fully automated ($A_{\text{cv-aut}}$) and those with only a manually adjustable preset pressure ($A_{\text{cv-man}}$). The former are modeled as follows. They can be *active* or *closed* and we model them as *unidirectional* elements, i.e., $q_a \geq 0$. The capability of reducing the inflow pressure is modeled by a continuous variable Δ_a with lower bound $\Delta_a^- \geq 0$ and upper bound $\Delta_a^+ \geq \Delta_a^-$. With this notation, our model of an automated control valve reads

$$a \text{ is active} \implies p_v = p_u - \Delta_a, \tag{9a}$$

$$a \text{ is closed} \implies q_a = 0. \tag{9b}$$

Since we modeled control valves as unidirectional elements, it is only possible to reduce the pressure in arc direction. However, gas flow against arc direction is often desired in a bypass mode. In order to model this situation, there is a so-called *bypass valve* in parallel to the control valve. Obviously, both the bypass and the control valve cannot be open at the same time. We refer to such restrictions that couple the discrete controls of a certain set of controllable elements as *subnetwork operation modes*; see Section 1.4. In addition, control valves often are located within larger entities called *control valve stations*. Due to station piping, filtering or measuring devices, there appear small pressure drops in the station. Thus, we model control valves always with suitably dimensioned in- and outflow resistors in order to account for these pressure drops; see Section 1.3.2.

A control valve with only manually adjustable preset pressure is represented by the following model:

$$p_v > p_a^{\text{set}} \implies q_a = 0, \tag{10a}$$

$$p_v < p_a^{\text{set}} \implies p_v = p_u, \tag{10b}$$

$$p_v = p_a^{\text{set}} \implies ((p_u \geq p_a^{\text{set}}) \wedge q_a \geq 0) \vee (q_a = 0 \vee (p_v = p_u)). \tag{10c}$$

Again, a specific MIP formulation can be found in [18].

1.3.5. *Compressor Machines.* A compressor machine $a \in A_{\text{cm}}$ increases the inlet gas pressure to a higher outlet pressure. Thus, compressor machines help to overcome the pressure loss in pipes and resistors and are essential for transporting gas over large distances.

For every compressor machine, we introduce a binary variable s_a that indicates whether the machine is active or not. This variable is coupled with the binary variable of the configuration in which the machine is operated; see Section 1.3.6. The compression results in a specific change of adiabatic enthalpy, $H_{\text{ad},a}$:

$$H_{\text{ad},a} = z_u T R_{\text{s}} \frac{\kappa}{\kappa - 1} \left(\left(\frac{p_v}{p_u} \right)^{\frac{\kappa-1}{\kappa}} - 1 \right) s_a \quad \text{for all } a \in A_{\text{cm}}. \tag{11}$$

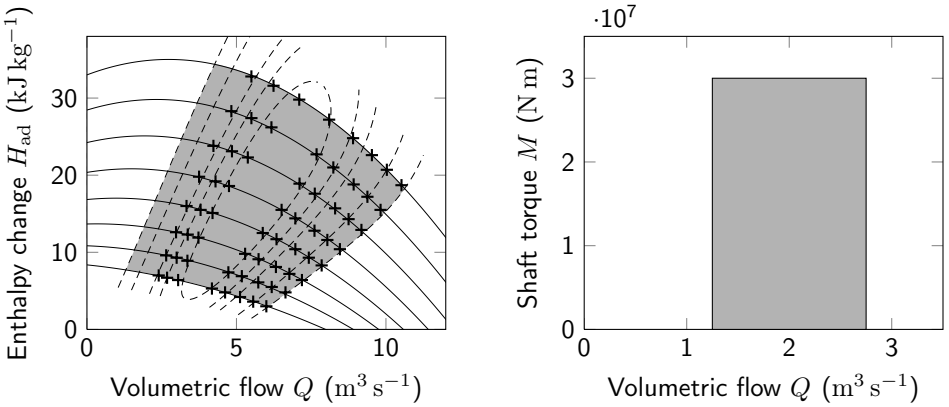

FIGURE 2. Characteristic diagrams of a turbo compressor (left) and a piston compressor (right). Feasible operating ranges are marked gray.

Here, $z_u = z(p_u, T)$ is the compressibility factor (1) under inflow conditions and κ is the isentropic exponent (assumed to be constant). Since the description of specific compressor types requires the flow to be given as a volumetric flow rate, we convert mass flow using the constraint

$$Q_a = (q_a/\rho_a)s_a \quad \text{for all } a \in A_{\mathrm{cm}}. \tag{12}$$

We distinguish between two different types of compressor machines: *turbo compressors* (A_{tc}) and *piston compressors* (A_{pc}), i.e., $A_{\mathrm{cm}} = A_{\mathrm{tc}} \cup A_{\mathrm{pc}}$.

Turbo compressors are modeled by so-called characteristic diagrams in $(Q_a, H_{\mathrm{ad},a})$-space; see Figure 2 (left). The curves of the diagram are defined using biquadratic and quadratic polynomials, $F_2(x, y; A)$ and $F_1(z; b)$, whose coefficients A and b are obtained from least-squares fits for given measurements of the compressor (crosses in Figure 2):

$$F_2(x,y;A) = \begin{pmatrix} 1 \\ x \\ x^2 \end{pmatrix}^T \begin{bmatrix} a_{00} & a_{01} & a_{02} \\ a_{10} & a_{11} & a_{12} \\ a_{20} & a_{21} & a_{22} \end{bmatrix} \begin{pmatrix} 1 \\ y \\ y^2 \end{pmatrix}, \quad F_1(z;b) = \begin{pmatrix} b_0 \\ b_1 \\ b_2 \end{pmatrix}^T \begin{pmatrix} 1 \\ z \\ z^2 \end{pmatrix}.$$

The isolines of speed $n_a \in [n_a^-, n_a^+]$ (solid) and adiabatic efficiency $\eta_{\mathrm{ad},a} \in [0, 1]$ (dashed) are given by

$$H_{\mathrm{ad},a} = F_2(Q_a, n_a; A_a^{H_{\mathrm{ad}}})s_a, \quad \eta_{\mathrm{ad},a} = F_2(Q_a, n_a; A_a^{\eta_{\mathrm{ad}}})s_a. \tag{13}$$

A compressor's *operating range* (gray area) is bounded by the isolines of minimal and maximal speeds $n_a^{\pm}$, by the *surgeline* (left), and by the *chokeline* (right),

$$H_{\mathrm{ad},a} \le F_1(Q_a; b_a^{\mathrm{surge}})s_a, \quad H_{\mathrm{ad},a} \ge F_1(Q_a; b_a^{\mathrm{choke}})s_a. \tag{14}$$

A piston compressor $a \in A_{\mathrm{pc}}$ is also modeled by a characteristic diagram; see Figure 2 (right). The feasible operating range of a piston compressor is given in (Q_a, M_a)-space, where

$$M_a = \frac{V_{\mathrm{o},a} H_{\mathrm{ad},a}}{2\pi\eta_{\mathrm{ad},a}} \rho_u s_a, \tag{15}$$

is the shaft torque. Here, $V_{\mathrm{o},a}$ is the operating volume of the machine that also defines, together with given minimal and maximal speed values, lower and upper bounds on the volumetric flow

$$s_a V_{\mathrm{o},a} n_a^- \le Q_a \le s_a V_{\mathrm{o},a} n_a^+. \tag{16}$$

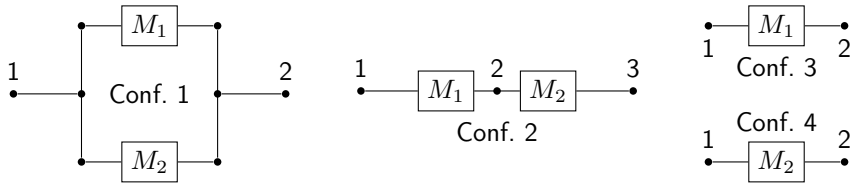

FIGURE 3. Complete set of possible configurations of a compressor group with two machines (a real station may offer only a subset).

Finally, the upper bound for M_a can be given explicitly or implicitly (depending on the specific machine) by

$$0 \leq \begin{cases} s_a(\varepsilon_a^+ p_u - p_v), \\ s_a(\Delta p_a^+ + p_u - p_v), \text{ or} \\ s_a(M_a^+ - M_a). \end{cases} \tag{17}$$

1.3.6. *Compressor Groups.* Compressor groups contain a certain number of compressor machines that can be operated in three different ways: *closed*, *bypass mode* and *active*. If active, they can be operated in one out of a finite number of so-called *configurations*, where we define a configuration to be a serial combination of parallel arrangements of compressor machines; see Figure 3 for all possible configurations of a group hosting two machines. At parallel arrangements, the gas flow divides upon the parallel machines and all parallel machines have to compress the gas to a unique outflow pressure. In order to control the state of the compressor group we introduce a vector of binary variables containing a binary variable for each state that indicates whether the state is active or not. In addition, the value of the binary variable of a specific compressor machine equals the value of the binary variable of the configuration in which the machine is hosted.

As it was the case for control valves (see Section 1.3.4), we model compressor groups as unidirectional elements, i.e., the mass flow has to be nonnegative and the pressure can only be increased in arc direction. Since backward flow is possible in bypass mode, an additional bypass valve is present and we model their interplay by subnetwork operation modes; see Section 1.4. Pressure losses due to station piping etc. are again modeled by resistors located at the tail and head of the station.

1.4. **Subnetwork Operation Modes.** We now describe the modeling of subnetwork operation modes. Let $\mathcal{S}$ denote the set of subnetworks with given operation modes, where each subnetwork $S \in \mathcal{S}$ is a triple $S = (A_S, \mathcal{M}_S, f_S)$ of the subnetwork's elements A_S, possible operation modes $\mathcal{M}_S \subseteq \{0,1\}^{A_S}$, and a mapping $f_S : A_S \times \mathcal{M}_S \to \{-1, 0, 1\}$ defined by

$$f_S(a, m) = \begin{cases} -1 & \text{if gas flows from } v \text{ to } u \text{ in operation mode } m, \\ 0 & \text{if the flow direction on } a \text{ is undefined in operation mode } m, \\ 1 & \text{if gas flows from } u \text{ to } v \text{ in operation mode } m. \end{cases}$$

We now introduce binary variables $s_m \in \{0,1\}$ for all $m \in \mathcal{M}_S$ and $S \in \mathcal{S}$ and model that for each subnetwork *exactly one* operation mode has to be chosen:

$$\sum_{m \in \mathcal{M}_S} s_m = 1 \quad \text{for all } S \in \mathcal{S}. \tag{18}$$

Further, a subnetwork element $a \in A_S$ may only be open (closed) if it has been declared to be open (closed) in the selected operation mode:

$$\sum_{m \in \mathcal{M}_S} m_a s_m \geq s_a \qquad \text{for all } S \in \mathcal{S}, a \in A_S, \tag{19a}$$

$$\sum_{m \in \mathcal{M}_S} (1 - m_a)\, s_m \geq (1 - s_a) \qquad \text{for all } S \in \mathcal{S}, a \in A_S. \tag{19b}$$

Note that $m_a \in \{0,1\}$ denotes the state (open/closed) of arc $a \in A_S$ in decision $m \in \{0,1\}^{A_S}$. Finally, if an operation mode specifies flow directions for some of the subnetwork elements, we have to guarantee that these flow directions are satisfied:

$$\left(1 + \sum_{(a,m) \in A_S \times \mathcal{M}_S} f_S(a,m) s_m\right) q_a^+ \geq q_a \qquad \text{for all } S \in \mathcal{S}, a \in A_S, \tag{20a}$$

$$\left(1 - \sum_{(a,m) \in A_S \times \mathcal{M}_S} f_S(a,m) s_m\right) q_a^- \leq q_a \qquad \text{for all } S \in \mathcal{S}, a \in A_S. \tag{20b}$$

1.5. **Heat Power Supply and Demand.** We now extend the model described so far in order to be able to incorporate heat power supply and demand as well as mixing of different gas compositions. For doing so, we introduce variables for the heat power P_u at all entry and exit nodes $u \in V_+ \cup V_-$, for the calorific value $H_{\mathrm{c},u}$ at all nodes $u \in V$, and for the calorific value $H_{\mathrm{c},a}$ at all arcs $a \in A$.

For entries and exits, the heat power is fixed to values $\bar{P}_u$ given from contracts:

$$P_u = \bar{P}_u \quad \text{for all } u \in V_+ \cup V_-. \tag{21}$$

We remark that the generalization from fixed heat powers to lower and upper bounds on the heat powers is readily possible. The supplied calorific values at entry nodes are also known and will be denoted by $H_{\mathrm{c},u}^{\mathrm{ext}}, u \in V_+$. Additionally, calorific value, heat power and mass flow are coupled by

$$P_u = q_u H_{\mathrm{c},u}^{\mathrm{ext}} \quad \text{for all } u \in V_+, \tag{22a}$$

$$P_u = q_u H_{\mathrm{c},u} \quad \text{for all } u \in V_- \cup V_0. \tag{22b}$$

Calorific values have to be mixed at each node of the network via

$$H_{\mathrm{c},u} = \frac{H_{\mathrm{c},u}^{\mathrm{ext}} q_u^{\mathrm{ext}} + \sum_{a \in \mathcal{I}(u)} H_{\mathrm{c},a} |q_a|}{q_u^{\mathrm{ext}} + \sum_{a \in \mathcal{I}(u)} |q_a|} \quad \text{for all } u \in V, \tag{23}$$

where we define $H_{\mathrm{c},u}^{\mathrm{ext}} = q_u^{\mathrm{ext}} = 0$ for all inner and exit nodes and $q_u^{\mathrm{ext}} = q_u$ at entry nodes. Finally, all mixed node quantities are propagated onto all outflow arcs, i.e.,

$$H_{\mathrm{c},a} = H_{\mathrm{c},u} \quad \text{for all } u \in V, a \in \mathcal{O}(u). \tag{24}$$

Since we assume that the molar mass m is constant in the whole network, Equation (23) takes a particularly simple form. In the case of non-constant molar mass, we may not mix weighted by mass flows but by molar flows $\hat{q} = |q|/m$.

From this model together with (3) it follows that heat power supplies at entries are given by nonnegative values ($\bar{P}_u \geq 0$) and that heat power demands at exits are given by nonpositive values ($\bar{P}_u \leq 0$).

1.6. **Model Summary.** We now collect all component models and state the feasibility problem that we solve in the following. The vector of all pressure variables is denoted by p, and the vector of all mass flow variables by q. All calorific values are summarized in the vector H_{c} and all power values in the vector P. Furthermore, the continuous variables of control valves, compressor machines, and resistors are

collected in the vectors x_{cv}, x_{cm}, and x_{rs} and all binary variables are condensed in the vector s. With this notation, our feasibility problem reads

$$\begin{aligned}
\text{Exists} \quad & (p, q, H_{\mathrm{c}}, P, x_{\mathrm{cv}}, x_{\mathrm{cm}}, x_{\mathrm{rs}}, s) && \text{(25a)}\\
\text{s.t.} \quad & \text{pressure and flow bounds: (2), (4);} && \text{(25b)}\\
& \text{mass flow conservation: (3);} && \text{(25c)}\\
& \text{pipes: (5);} && \text{(25d)}\\
& \text{resistors: (6), (7);} && \text{(25e)}\\
& \text{valves: (8);} && \text{(25f)}\\
& \text{control valves: (9), (10);} && \text{(25g)}\\
& \text{compressors: (11)–(17);} && \text{(25h)}\\
& \text{subnetwork operation modes: (18)–(20);} && \text{(25i)}\\
& \text{heat power: (21)–(24)?} && \text{(25j)}
\end{aligned}$$

The submodel (25a)–(25i) is a feasibility problem for gas transport networks that is only based on flow and that is well studied in the literature. The constraints (25j) extend this standard model by additional bilinear and nonsmooth pooling-type constraints that allow to consider heat power supply and demand. The nonsmoothness appears in the mixing equations (23) since the in- and outflow arcs $\mathcal{I}(u)$ and $\mathcal{O}(u)$ are not known a priori. The complete problem (25) is a mixed-integer nonlinear, nonconvex and nonsmooth feasibility problem and is thus NP-hard. Note further that it contains a special instance of a pooling problem, which is also NP-hard.

Lemma 1.1. *Suppose that constraints* (3), (21), (22), *and* (24) *hold, m is constant, and set*

$$P_a = q_a H_{\mathrm{c},a} \quad \textit{for all } a \in A. \tag{26}$$

Then condition (23) *is satisfied if and only if*

$$\sum_{a \in \mathcal{O}(u)} |P_a| - \sum_{a \in \mathcal{I}(u)} |P_a| = P_u \quad \textit{for all } u \in V. \tag{27}$$

Proof. Let $u \in V$ be an arbitrary node. Then the following equality holds:

$$\begin{aligned}
\sum_{a \in \mathcal{O}(u)} |P_a| - \sum_{a \in \mathcal{I}(u)} |P_a| &= \sum_{a \in \mathcal{O}(u)} H_{\mathrm{c},a} \, |q_a| - \sum_{a \in \mathcal{I}(u)} H_{\mathrm{c},a} \, |q_a| && \text{with Eq. (26)}\\
&= H_{\mathrm{c},u} \sum_{a \in \mathcal{O}(u)} |q_a| - \sum_{a \in \mathcal{I}(u)} H_{\mathrm{c},a} \, |q_a| && \text{with Eq. (24)}\\
&= H_{\mathrm{c},u} q_u + H_{\mathrm{c},u} \sum_{a \in \mathcal{I}(u)} |q_a| - \sum_{a \in \mathcal{I}(u)} H_{\mathrm{c},a} \, |q_a| && \text{with Eq. (3).}
\end{aligned}$$

Condition (23) is equivalent to

$$H_{\mathrm{c},u} \sum_{a \in \mathcal{I}(u)} |q_a| - \sum_{a \in \mathcal{I}(u)} H_{\mathrm{c},a} \, |q_a| = H_{\mathrm{c},u}^{\mathrm{ext}} q_u^{\mathrm{ext}} - H_{\mathrm{c},u} q_u^{\mathrm{ext}}.$$

From these equations it follows that the claim of the lemma is equivalent to the following equation:

$$H_{\mathrm{c},u}^{\mathrm{ext}} q_u^{\mathrm{ext}} - H_{\mathrm{c},u} q_u^{\mathrm{ext}} = P_u - H_{\mathrm{c},u} q_u. \tag{28}$$

For $u \in V_+$ it holds that $q_u^{\mathrm{ext}} = q_u$. Equation (28) follows then from equation (22a). For $u \in V_- \cup V_0$ it holds that $q_u^{\mathrm{ext}} = 0$ and equation (28) follows from equation (22b). □

The lemma tells us that we can replace the mixing equations in problem (25) by additional heat power constraints at arcs (26) and additional heat power balance equations at nodes (27). Thus, problem (25) is equivalent to

$$\begin{aligned}
\text{Exists} \quad & (p, q, H_{\mathrm{c}}, P, x_{\mathrm{cv}}, x_{\mathrm{cm}}, x_{\mathrm{rs}}, s) && \text{(29a)}\\
\text{s.t.} \quad & \text{pressure and flow bounds: } (2), (4); && \text{(29b)}\\
& \text{mass flow conservation: } (3); && \text{(29c)}\\
& \text{pipes: } (5); && \text{(29d)}\\
& \text{resistors: } (6), (7); && \text{(29e)}\\
& \text{valves: } (8); && \text{(29f)}\\
& \text{control valves: } (9), (10); && \text{(29g)}\\
& \text{compressors: } (11)\text{–}(17); && \text{(29h)}\\
& \text{subnetwork operation modes: } (18)\text{–}(20); && \text{(29i)}\\
& \text{heat power: } (21), (22), (24), (26), (27). && \text{(29j)}
\end{aligned}$$

Note that the vector P now also contains all power variables at arcs.

2. A mixed-integer linear relaxation

The nonconvex MINLP (29) can be tackled by different approaches. Obviously, one could try to solve the MINLP by means of a generic MINLP solver. Unfortunately, state-of-the-art MINLP solvers for nonconvex problems are not applicable for our desired problem size as it is computationally demonstrated even for much smaller instances in [27]. An alternative method to tackle problem (29) is based on the fundamental idea to set up an a priori mixed-integer linear relaxation [13].

In Section 2.1 we summarize a technique to derived such a relaxation by means of piecewise linear approximations to nonlinear univariate functions. Subsequently, we present an algorithm to compute piecewise linear approximations with a minimal number of line segments to obtain corresponding relaxations with as few binary variables as possible. In Section 2.2 we then explain how the large number of nonlinear relations resulting from the squares of pressures can be further reduced.

2.1. Optimal Piecewise Linear Relaxations.

To obtain a mixed-integer linear relaxation, in a first step, we replace each occurrence of an expression $f(x)$ in model (29), where f is an univariate nonlinear function, by a newly introduced variable y. Then, we approximate $f(x)$ by a piecewise linear function $\phi(x)$, such that for $\varepsilon > 0$ the approximation satisfies $|f(x) - \phi(x)| \leq \varepsilon$ for all relevant x. Next, we introduce another variable y' for the approximate value of $f(x)$, with $\phi(x) - \varepsilon \leq y' \leq \phi(x) + \varepsilon$, and add the constraint $y = y'$ to our model. Since $f(x) - \varepsilon \leq \phi(x) \leq f(x) + \varepsilon$, any feasible point to the original MINLP is still feasible and we obtain a relaxation.

The resulting piecewise linear approximations are typically still nonconvex. However, any piecewise linear function can be modeled by using additional binary variables and linear constraints and thus our relaxation of problem (29) can be formulated as an MIP. An important fact is that the resulting MIPs in practice can be solved comparatively faster than MINLPs; see [27] or [18].

The drawbacks of such an approach are that MIP-based relaxations suffer from the curse of dimensionality and the solution of an MIP relaxation might only satisfy the constraints up to a tolerance of ε. The first disadvantage is due to the fact that the size of the MIP formulations, and especially the number of binary variables, depend on the number of pieces of the piecewise linear functions. In order to

Algorithm 1 : Computation of a piecewise linear approximation with error at most ε and a minimum number of pieces.

Input : A continuous function $f : [a, b] \to \mathbb{R}$, an upper bound on the overall error $\varepsilon > 0$, and an upper bound on the minimal number of pieces k^+.

Output : An optimal piecewise linear approximation ϕ^* of f on $[a, b]$, i.e., a piecewise linear approximation with overall approximation error $\varepsilon^* \leq \varepsilon$ and a minimum number of pieces k^*.

1 Initialize the lower bound k^- on k^* to $k^- \leftarrow 0$.
2 **while** $k^+ - k^- > 1$ **do**
3 Choose some k with $k^- < k < k^+$.
4 Choose arbitrary points $a = \tilde{x}_0 < \tilde{x}_1 < \cdots < \tilde{x}_k = b$.
5 Compute $\tilde{\varepsilon}_i = \min_{\alpha_i, \beta_i \in \mathbb{R}} \max_{x \in [\tilde{x}_{i-1}, \tilde{x}_i]} |f(x) - (\alpha_i x + \beta_i)|$ for $i = 1, \ldots, k$ and let $\phi_{k,i}(x) = \alpha_i x + \beta_i$ be the solution.
6 **while** $\min_{i=1,\ldots,k} \tilde{\varepsilon}_i < \max_{i=1,\ldots,k} \tilde{\varepsilon}_i$ **do**
7 Compute $\tilde{c}_i = \tilde{\varepsilon}_i / (\tilde{x}_i - \tilde{x}_{i-1})^2$ for $i = 1, \ldots, k$.
8 Solve the system of equations $x_0 = a, x_k = b, \tilde{c}_i (x_i - x_{i-1})^2 = \varepsilon$, $i = 1, \ldots, k$ for the unknowns $x_0, \ldots, x_k, \varepsilon$. Let $\tilde{x}$ be the solution.
9 Compute $\tilde{\varepsilon}_i = \min_{\alpha_i, \beta_i \in \mathbb{R}} \max_{x \in [\tilde{x}_{i-1}, \tilde{x}_i]} |f(x) - (\alpha_i x + \beta_i)|$ and let $\phi_{k,i}(x) = \alpha_i x + \beta_i$ be the solution for $i = 1, \ldots, k$.
10 **if** $\min_{i=1,\ldots,k} \tilde{\varepsilon}_i > \varepsilon$ **then**
11 Update $k^- \leftarrow k$.
12 **if** $\max_{i=1,\ldots,k} \tilde{\varepsilon}_i \leq \varepsilon$ **then**
13 Update $k^+ \leftarrow k$, $\phi^+ \leftarrow \phi_k$, and $\varepsilon^+ \leftarrow \max_{i=1,\ldots,k} \tilde{\varepsilon}_i$.
14 Set $k^* \leftarrow k^+$, $\phi^* \leftarrow \phi^+$, and $\varepsilon^* \leftarrow \varepsilon^+$.
15 **return** k^*, ϕ^*, and ε^*

compensate for this drawback as much as possible, we are interested in piecewise linear approximations to nonlinear functions with a minimal number of pieces.

To determine a piecewise linear approximation $\phi^*(x)$ of a univariate continuous function $f(x)$ with approximation error ε^* and a minimal number of k^* pieces that satisfies an a priori error tolerance $\varepsilon \geq \varepsilon^* > 0$ we make use of Algorithm 1 proposed in [22]. It can be summarized as follows: In the inner loop a piecewise linear approximation ϕ_k with minimal overall maximum error for a fixed number of k pieces is determined. The key ingredient to solve the optimization problems in Steps 5 and 9 is the so-called minimax approximation theory; see, e.g., [28, 35]. One aim of the minimax theory is to find the unique polynomial of degree at most n (here $n = 1$ to obtain linear approximations) that minimizes the maximum approximation error to a continuous univariate nonlinear function. The most famous algorithm to construct such a minimax approximation and hence a possibility to solve the optimization problems is known as Remez' Algorithm [29]. During the inner loop, the algorithm estimates new breakpoints $a = \tilde{x}_0 \leq \tilde{x}_1 \leq \cdots \leq \tilde{x}_{k-1} \leq \tilde{x}_k = b$ based on an approximation problem and updates them by the exact evaluation of the minimax approximation on the intervals resulting from these breakpoints. The fact that the piecewise linear approximation obtained after termination of the inner loop is the maximum-error minimizer for k pieces is an immediate consequence of the following theorem:

Theorem 2.1 ([19])**.** *Let $f : [a, b] \to \mathbb{R}$ be a continuous function and let $p = (p_i : [x_{i-1}, x_i] \to \mathbb{R})_{i=1}^{k}$ and $p' = \left(p'_i : [x'_{i-1}, x'_i] \to \mathbb{R}\right)_{i=1}^{k'}$, with $k' \leq k$ be two*

piecewise minimax approximations of degree n of f over $[a,b]$ with respective errors $\varepsilon_i := \max_{x\in[x_{i-1},x_i]}|p_i(x)-f(x)|$ and $\varepsilon'_i := \max_{x\in[x'_{i-1},x'_i]}|p'_i(x)-f(x)|$. Then

$$\min\{\varepsilon_i : i=1,\dots,k\} \le \max\{\varepsilon'_i : i=1,\dots,k'\}.$$

The outer loop in Algorithm 1 is a one-dimensional search over the number of pieces k while maintaining a valid bracketing $k^- < k^* \le k^+$ of the minimum number of pieces k^*. A simple adaptive refinement algorithm could be applied for the purpose of determining the initial upper bound k^+: Start with only two breakpoints and compute the minimax approximation on the corresponding interval. If the approximation error tolerance is not satisfied then insert a new breakpoint, e.g., at the midpoint or the point where the maximum error is attained. Then iteratively recompute the minimax approximation on each piece until the desired error tolerance is satisfied.

Unfortunately, there are no convergence results for this algorithm known yet, but the algorithm works well for the functions appearing in gas network models. It is known that the algorithm might fail in the special case when some $\tilde{c}_i = 0$. However, for most functions this is impossible, so there is still hope for a convergence result for the other cases. In [26] a different algorithm is proposed, for which convergence can be assured for a suitable parameter choice. Nonetheless this choice leads to a slow algorithm in practice and hence different parameters are chosen.

The following theorem summarizes the main theoretical property of Algorithm 1:

Theorem 2.2 ([19, 22])**.** *If Algorithm 1 terminates, it returns a piecewise linear approximation ϕ^* with a minimal number of pieces k^* such that the maximum error over each piece is minimized and is equal to ε^*. Moreover at any time a lower bound k^- and an upper bound k^+ on the minimal number of pieces is provided.*

Since the nonlinear functions appearing in Equations (5) and (6) are separable we can apply the described procedure in a straight forward manner to the individual nonlinear terms.

To model the resulting discontinuous piecewise linear approximations with k line segments—given by a sequence of $2k+1$ breakpoints $(x_0,y_{0,r}),(x_1,y_{1,l}),(x_1,y_{1,r}),\dots,(x_{k-1},y_{k-1,l}),(x_{k-1},y_{k-1,r}),(x_k,y_{k,l})$ and an approximation error ε—in terms of mixed-integer linear constraints, we apply the so-called disaggregated incremental model:

$$x = x_0 + \sum_{i=1}^{k}(x_i - x_{i-1})\delta_i, \tag{30a}$$

$$y = y_{0,r} + \sum_{i=1}^{k}(y_{i,l} - y_{i-1,r})\delta_i + \sum_{i=1}^{k-1}(y_{i,r} - y_{i,l})z_i + e, \tag{30b}$$

$$z_i \in \{0,1\}, \quad \delta_{i+1} \le z_i \le \delta_i \quad \text{for } i=1,\dots,k-1, \tag{30c}$$

$$0 \le \delta_1, \quad \delta_k \le 1, \quad -\varepsilon \le e \le \varepsilon. \tag{30d}$$

For a description of this modeling technique, as well as for further details on the theory of piecewise minimax approximations, we refer to [22].

Since we explicitly refer to the additional variables introduced for the squares of pressures in the following, we denote them by π and π'. In particular π_u and π_v are the respective variables occurring in the linearized version of (5) and (6).

The nonconvex operating ranges of turbo compressors, see (13)–(14), are handled differently. As described in [18, Chapter 6], we replace each of these nonconvex sets by a convex superset and during branch-and-bound, we cut off any point outside the convexified operating range by a separating hyperplane.

2.2. **Reduction of Nonlinear Relations.** One drawback of the formulation above is the large number of nonlinear coupling equations resulting from the fact that we introduced variables for pressures and squares of pressures at each node. At many nodes either one of them is sufficient; in this case it is advantageous to remove the unnecessary variable and hence the approximation among them. There are some elements $(u, v) \in A$ that require variables p_u and p_v, we collect these in the set A_p, defined by $A_p := A_{\mathrm{cv}} \cup A_{\mathrm{cm}} \cup A_{\mathrm{rs}}$. Analogously we define the set A_π as $A_\pi := A_{\mathrm{pi}} \cup A_{\text{nl-rs}}$. For elements like short pipes and valves it is only necessary that at both ends the same type of variable is part of the model. The choice awarded by these latter elements makes it tempting to look for the optimal choice of introduced variables; optimal in the sense of yielding an easy to solve MIP. As a proxy for the difficulty of the resulting MIP, we use the number of binary variables needed to discretize the function $p_u \mapsto p_u^2$, which can be computed a priori. The resulting weight C_u is then used in the objective function of the integer program.

$$
\begin{aligned}
\min \quad & \sum_{u \in V} C_u \left(\alpha_u^p + \alpha_u^\pi\right) \\
\text{s.t.} \quad & \alpha_u^p + \alpha_v^\pi \geq 1 && \text{for all } (u,v) \in A \setminus (A_p \cup A_\pi)\,, \\
& \alpha_u^\pi + \alpha_v^p \geq 1 && \text{for all } (u,v) \in A \setminus (A_p \cup A_\pi)\,, \\
& \alpha_u^p + \alpha_u^\pi \geq 1 && \text{for all } u \in V, \\
& \alpha_u^p = \alpha_v^p = 1 && \text{for all } (u,v) \in A_p, \\
& \alpha_u^\pi = \alpha_v^\pi = 1 && \text{for all } (u,v) \in A_\pi, \\
& \alpha_u^p, \alpha_u^\pi \in \{0,1\} && \text{for all } u \in V.
\end{aligned}
$$

In our experiments the time to set up and solve this integer program is negligible, the resulting speed up, however, is not.

3. The Alternating Direction Method

The methods outlined in the previous section have been successfully used to solve gas transport problems without power constraints [5, 8, 10, 12, 13, 18, 27]. Experiments show that these techniques fail to yield satisfying results for the power constrained case. This is the reason why we apply a tailored version of an alternating direction method (ADM). The key idea is to reduce the power constrained model to a problem in which mixing does not appear due to fixed values of the calorific values. Solving this problem yields new discrete controls for the active network elements and according flow and pressure values. Afterwards, improved calorific values are computed for this fixed pressure-flow setting.

Classical ADMs are extensions of augmented Lagrangian methods. They are originally proposed in [14] and [9] in the context of nonlinear variational problems. A general presentation of the convergence theory of ADMs based on the augmented Lagrangian (ADMM) can be found in [1]. The special case of ADMs applied to convex objective functions $f(x, y)$ over disjoint constraint sets $x \in X, y \in Y$, is discussed in [37]. An extension to the case of biconvex f is given in [15]. Finally, [2] discusses applications of ADMMs in the broad area of machine learning and highlights the possibility of parallelization of ADMMs.

We now reformulate model (29) in order to be able to apply a tailored ADM to solve the problem. For this, we define

$$
\begin{aligned}
f_V &:= \left\| (\bar{P}_u - q_u H_{\mathrm{c},u})_{u \in V_+ \cup V_-} \right\|_1, \\
f_A &:= \left\| (P_a - q_a H_{\mathrm{c},a})_{a \in A} \right\|_1, \\
f_\pi &:= \left\| (\pi'_u - \pi_u)_{u \in A_p \cap A_\pi} \right\|_1
\end{aligned}
$$

Algorithm 2 : The Alternating Direction Method.

Input : Termination tolerance $\tau > 0$

Set $k = 0$.

Compute initial values $p^k, q^k, H_c^k, P^k, x_{cv}^k, x_{cm}^k, x_{rs}^k, x_{lin}^k, s^k, s_{lin}^k$.

while $f^k > \tau$ **do**

  Solve (31) for fixed values $H_c = H_c^k$, yielding the new iterates p^{k+1}, q^{k+1}, P^{k+1}, x_{cv}^{k+1}, x_{cm}^{k+1}, x_{rs}^{k+1}, x_{lin}^{k+1}, s^{k+1}, and s_{lin}^{k+1}.

  Solve (31) for fixed values $p = p^{k+1}$, $q = q^{k+1}$, $P = P^{k+1}$, $x_{cv} = x_{cv}^{k+1}$, $x_{cm} = x_{cm}^{k+1}$, $x_{rs} = x_{rs}^{k+1}$, $x_{lin} = x_{lin}^{k+1}$, $s = s^{k+1}$, and $s_{lin} = s_{lin}^{k+1}$, yielding the new iterate H_c^{k+1}.

  Set $k \leftarrow k + 1$.

and reformulate model (29) by removing the heat power constraints on nodes and arcs as well as the π-π' coupling constraints of the linearization (see Section 2) from the set of constraints and penalize their violation in the objective function by weighted ℓ_1 penalty terms. Due to the linearization techniques described in Section 2, additional continuous and binary auxiliary variables (summarized in the vectors x_{lin} and s_{lin}) have to be added to the problem. The resulting optimization model reads

$$\begin{aligned}
\min \quad & f := \lambda_V f_V + \lambda_A f_A + \lambda_\pi f_\pi && \text{(31a)}\\
\text{s.t.} \quad & \text{pressure and flow bounds: (2), (4);} && \text{(31b)}\\
& \text{mass flow conservation: (3);} && \text{(31c)}\\
& \text{pipes (linearized): (5);} && \text{(31d)}\\
& \text{resistors (linearized): (6), (7);} && \text{(31e)}\\
& \text{valves: (8);} && \text{(31f)}\\
& \text{control valves: (9), (10);} && \text{(31g)}\\
& \text{compressors (linearized): (11)–(17);} && \text{(31h)}\\
& \text{subnetwork operation modes: (18)–(20);} && \text{(31i)}\\
& \text{heat power: (24), (27).} && \text{(31j)}
\end{aligned}$$

The main idea of the ADM is the following: First solve (31) for fixed calorific value variables. This nonconvex MINLP is comparable to standard gas transport models that are based on flow and for which a robust solution framework has been developed in the recent past [18, 27]. We solve this MINLP using the linear relaxation techniques described in Section 2; see also [12, 13]. Next, we fix all discrete and continuous variables except for the calorific value variables. By this, the resulting model reduces to an LP that can be solved by any general-purpose LP solver. A formal statement of the algorithm is given in Algorithm 2.

For the algorithm above convergence can be shown. The convergence results are variants of results discussed in [37] and [15]. To simplify notation, we consider the following abstract setup,

$$\min\{f(x, y) : x \in X, y \in Y\},$$

where X and Y are closed sets. We further assume that f is continuous and use the abbreviation $z = (x, y)$. If we denote the feasible region of (29) by Ω, we can define

X and Y as

$$X := \{(p, q, P, x_{\text{cv}}, x_{\text{cm}}, x_{\text{lin}}, s, s_{\text{lin}}) : (p, q, H_{\text{c}}, P, x_{\text{cv}}, x_{\text{cm}}, x_{\text{lin}}, s, s_{\text{lin}}) \in \Omega\},$$
$$Y := \{H_{\text{c}} : (p, q, H_{\text{c}}, P, x_{\text{cv}}, x_{\text{cm}}, x_{\text{lin}}, s, s_{\text{lin}}) \in \Omega\}.$$

In this notation Algorithm 2 proceeds as follows: We start with an initial point (x^0, y^0) and iterate the following two steps:

(1) Compute $x^{i+1} \leftarrow \arg\min\{f(x, y^i) : x \in X\}$,
(2) compute $y^{i+1} \leftarrow \arg\min\{f(x^{i+1}, y) : y \in Y\}$.

Algorithm 2 does not always converge to a local minimum of f. To formulate convergence results a useful weaker concept is the notion of a partial minimum:

Definition 3.1 (partial minimum)**.** Let X, Y be sets and $f : X \times Y \to \mathbb{R}$. Then (x^*, y^*) is called a *partial minimum* of f, if

$$f(x^*, y^*) \le f(x, y^*) \quad \text{for all } x \in X \quad \text{and} \quad f(x^*, y^*) \le f(x^*, y) \quad \text{for all } y \in Y.$$

The following convergence result can be proved directly; see [15]. Here $\Theta(\bar{x}, \bar{y})$ denotes the possible iterates starting from point $(\bar{x}, \bar{y})$, that is

$$\Theta(\bar{x}, \bar{y}) = \{(x^*, y^*) : \forall x \in X. f(x^*, \bar{y}) \le f(x, \bar{y}); \forall y \in Y. f(x^*, y^*) \le f(x^*, y)\}.$$

Theorem 3.2. *Let $\{(x^i, y^i)\}_{i=0}^{\infty}$ be a sequence with $(x^{i+1}, y^{i+1}) \in \Theta(x^i, y^i)$. Assume that the solution of the first optimization problem is always unique. Then every convergent subsequence of $\{(x^i, y^i)\}_{i=0}^{\infty}$ converges to a partial minimum. For two limit points z, z' of such subsequences it holds that $f(z) = f(z')$.*

Partial minimality is obviously a rather weak concept. As our problem is nonconvex, we cannot, in general, expect to achieve convergence to a global minimum with our alternating approach. Even local optimality seems to be out of reach as first order information is not available in our setting. We can, however, show convergence to a stationary point only assuming differentiability of f.

The following result is a weaker version of a result by Wendell and Hurter [37, Proposition 1]. In our case we may not assume that f is convex, which allows us only to conclude convergence to a stationary point.

Theorem 3.3. *Let X, Y be closed sets. Assume that $f : X \times Y \to \mathbb{R}$ is continuously differentiable. If (x^*, y^*) is a partial minimum of f then it is a stationary point, i.e., it satisfies*

$$\nabla f(x^*, y^*)^T d \ge 0 \quad \textit{for all } d \in T_{X \times Y}(x^*, y^*),$$

where $T_{X \times Y}(x^*, y^*)$ denotes the tangent cone of $X \times Y$ at (x^*, y^*); see [24].

Even for simple nondifferentiable functions like $|xy - c|$ with $c > 0$ such a result does not hold. Moreover, even using generalized notions of differentiability as, e.g., Clarke's generalized gradient (see [3]), we cannot show analogous results as we cannot combine the x- and y-components of such a generalized gradient to a generalized gradient for the full function f. This corresponds to the fact that for functions that only have directional derivatives, we can in general not compute the directional derivative only using the partial derivatives.

Furthermore, it can easily be seen that there exist partially optimal values for our problem that are not locally optimal: The objective function of (31) consists of terms like $|xy - c| - |x - y|$, for which any point (x, y) with $x = y$ is partially optimal but only $x = y = \sqrt{c}$ is locally optimal. Thus, we cannot expect stronger results than convergence to partially optimal values for our specific application.

4. Computational Results

In this section, we present computational evidence that our algorithm is able to solve large-scale real-world power constrained gas transportation problems. We will see that the running times of our algorithm are short enough to fit the requirements of a productive network planning tool.

We proceed with a brief description of the computational setup, a description of the test instances, and a discussion of the numerical results obtained on these instances.

4.1. **Computational Setup.** As already described, the ADM algorithm alternately solves an MIP and an LP model in each iteration. Both types of models are solved with Gurobi 5.6.3 [16] using only a single thread during branch-and-cut. All computations presented in this section have been performed on a computer with two Six-Core AMD Opteron(tm) 2435Q CPUs with 2.6 GHz and with 64 GB of main memory.

The major part of the computing time amounts to the solution of the MIPs. Since the complexity of the MIP models heavily depends on the size of the domains of the piecewise linear approximations, the actual model construction is preceded by a bound strengthening step; see [11]. Moreover, our experience shows that it is not required to solve the MIP models to optimality. Instead, we terminate the solution process after 2000 branch-and-bound nodes have been processed.

Further, it turned out that it is often computationally expensive to find an initial feasible solution of the MIP. To overcome this issue, we apply a zero-objective heuristic in the first iteration, i.e., the MIP gets initially solved without applying any objective function at all. From iteration 2 on, the objective function (31a) is added to the MIP model.

Also from iteration 2 on, we extend Gurobi's branch-and-cut algorithm by two primal heuristics that aim to improve the incumbent solution. The first one is a RINS heuristic [4] with minor problem-specific adaptations. The second one is a fixed-flow heuristic that is called whenever a new incumbent solution has been found. In the fixed-flow heuristic a sub-MIP is solved, in which the flow variables are fixed to their values in the current incumbent solution.

4.2. **Test Instances.** In our computations we aim to solve validation of nominations problems for Germany's largest gas transport network operated by the Open Grid Europe GmbH. The network is made up of two subnetworks, one for the transport of low-calorific gas (L-gas) with calorific values ranging from 34 $\mathrm{MJ/Nm^3}$ to 36 $\mathrm{MJ/Nm^3}$, and one for the transport of high calorific gas (H-gas) with calorific values from 36 $\mathrm{MJ/Nm^3}$ to 44 $\mathrm{MJ/Nm^3}$. From the network operators we are given 33 realistic nominations for the L-gas network with an overall supply ranging from 30 GW to 90 GW, and 30 instances for the H-gas network, where the amounts of transported gas range from 120 GW to 250 GW.

The L-gas network shown in Figure 4 consists of 4189 nodes, whereof 12 are entries and 964 are exits. These nodes are connected by altogether 4460 arcs, which subdivide into 3550 pipes, 349 short pipes, 28 resistors, 401 valves, 120 control valves, and 12 compressor groups. The H-gas network, see Figure 5, consists of 2735 nodes connected by 3074 arcs. Among the nodes, 45 are entries and 429 are exits. The arc set subdivides into 1747 pipes, 511 short pipes, 85 resistors, 545 valves, 145 control valves, and 41 compressor groups. Note that even though the L-gas network is larger than the H-gas network, the latter contains a larger number of controllable elements, i.e., valves, control valves, and compressor groups, making it harder to solve.

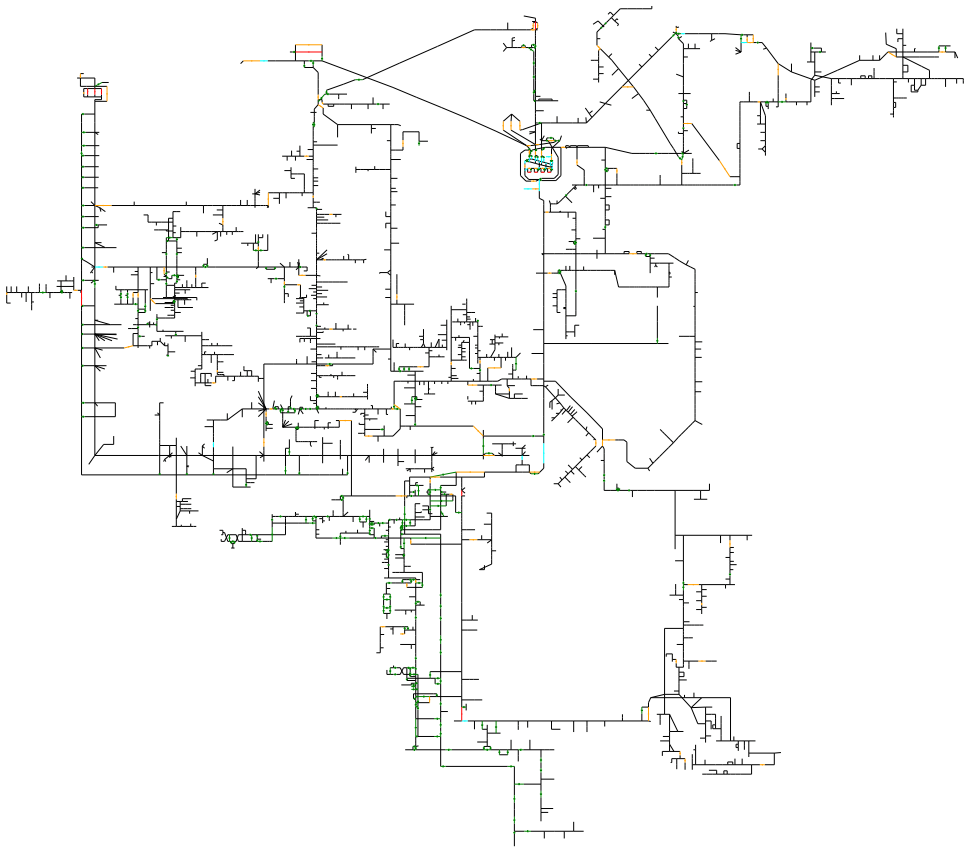

FIGURE 4. The L-gas network.

4.3. **Discussion.** The results for the L-gas network are presented in Table 1. For the H-gas network the results are summarized in Table 2. The first column in both tables indicates the nomination to be validated. By $\Delta_P \in \mathbb{R}^{|V_-|}$, with $\Delta_{P,u} := |P_u - \bar{P}_u|$ for all $u \in V_-$, we denote the difference in MW of the heat power P_u delivered to node u from the heat power demand $\bar{P}_u$. The maximum relative error is denoted by $\Delta_P^{\text{rel}} \in \mathbb{R}^{|V_-|}$, with $\Delta_{P,u}^{\text{rel}} := \Delta_{P,u}/\bar{P}_u$ for all $u \in V_-$. Next, $\Delta_{\text{mix}} \in \mathbb{R}^{|V|}$ denotes the violation of the mixing equation (23) in MW. The violation of the equations $p_u = \sqrt{\pi_u}$ measured in bar is denoted by $\Delta_{\pi,u}$ for all nodes u at which both a pressure and a squared pressure variable is required; see Section 2.2. Finally, the last two columns contain the number of ADM iterations (N), and the running time of the ADM algorithm in seconds.

The algorithm terminates as soon as $\|\Delta_\pi\|_\infty < 0.1\,\text{bar}$ and either $\|\Delta_P\|_\infty < 10\,\text{MW}$ and $\|\Delta_P^{\text{rel}}\|_\infty < 0.01$, or $\|\Delta_P\|_\infty < 0.5\,\text{MW}$ and $\|\Delta_P^{\text{rel}}\|_\infty < 0.15$. Furthermore, $\|\Delta_{\text{mix}}\|_\infty < 1\,\text{kW}$ has to be fulfilled and minor violations in power demand up to 100 kW per node are neglected with respect to the termination criterion.

To obtain the results given in Table 1 and 2, we chose the objective function coefficients as $\lambda_A = \lambda_V = 1$ and $\lambda_\pi = 0.01$ in Problem (31) and apply a limit of 10 to the number of ADM iterations.

As one might easily see, the results are not satisfying. Except for $\|\Delta_\pi\|_\infty < 0.1\,\text{bar}$ none of the termination criteria can be satisfied for any of the instances. Even worse, several experiments with other values for the objective function coefficients or higher values for the maximum number of ADM iterations led to similar results.

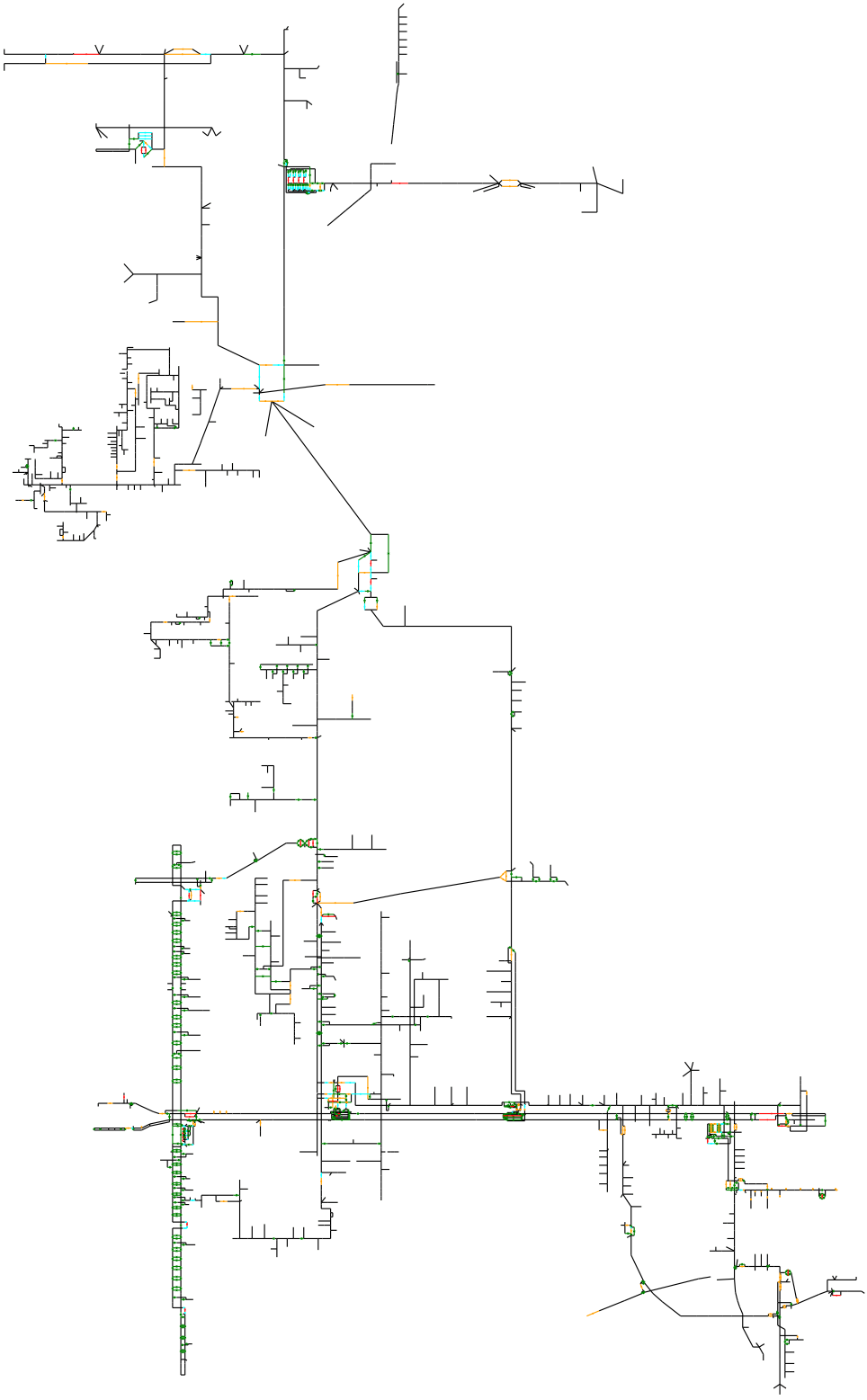

FIGURE 5. The H-gas network.

TABLE 1. Results on the L-gas instances.

Instance	$\|\Delta_P\|_\infty$	$\|\Delta_P^{\text{rel}}\|_\infty$	$\|\Delta_{\text{mix}}\|_\infty$	$\|\Delta_\pi\|_\infty$	N	Time
L-01	5.21×10^1	0.0730	9.95×10^2	0.05	10	13108
L-02	4.50×10^1	0.0730	2.23×10^2	0.00	10	13064
L-03	2.08×10^1	0.0730	1.17×10^2	0.00	10	10059
L-04	2.08×10^1	0.0730	2.45×10^2	0.00	10	13453
L-05	3.76×10^1	0.0730	4.34×10^2	0.00	10	14833
L-06	3.76×10^1	0.0730	4.50×10^2	0.00	10	13773
L-07	2.08×10^1	0.0730	1.53×10^2	0.20	10	12638
L-08	5.19×10^1	0.0723	1.50×10^2	0.00	10	15102
L-09	6.38×10^1	0.0730	4.38×10^2	0.13	10	15650
L-10	2.77×10^1	0.0730	4.53×10^2	0.00	10	11565
L-11	4.93×10^1	0.0728	1.50×10^2	0.00	10	7859
L-12	7.69×10^1	0.0740	5.01×10^2	0.00	10	15578
L-13	2.92×10^1	0.0730	7.25×10^2	0.00	10	19653
L-14	2.03×10^1	0.0730	2.08×10^2	0.00	10	10782
L-15	1.96×10^1	0.0730	5.01×10^2	0.00	10	14014
L-16	1.68×10^1	0.0702	5.11×10^2	0.00	10	6326
L-17	2.38×10^1	0.0730	6.25×10^2	0.00	10	12467
L-18	2.39×10^1	0.0730	6.30×10^2	0.00	10	10607
L-19	2.28×10^1	0.0720	7.50×10^2	0.00	10	19389
L-20	1.84×10^1	0.0720	6.28×10^2	0.00	10	13957
L-21	2.31×10^1	0.0730	6.12×10^2	0.00	10	15127
L-22	2.29×10^1	0.0730	6.24×10^2	0.00	10	15380
L-23	2.40×10^1	0.0721	6.27×10^2	0.00	10	9881
L-24	1.98×10^1	0.0702	1.76×10^2	0.00	10	14322
L-25	8.08	0.0680	5.09×10^2	0.00	10	9506
L-26	2.28×10^1	0.0730	6.70×10^2	0.00	10	11187
L-27	2.28×10^1	0.0700	6.23×10^2	0.00	10	12197
L-28	1.94×10^1	0.0730	1.71×10^2	0.00	10	6811
L-29	2.83×10^1	0.0730	6.25×10^2	0.00	10	8209
L-30	5.17×10^1	0.0727	2.16×10^2	0.00	10	12608
L-31	5.21×10^1	0.0726	1.02×10^3	0.31	10	17531
L-32	1.42×10^2	0.0730	2.51×10^2	0.00	10	17741
L-33	3.63×10^1	0.0730	4.61×10^2	0.00	10	15342

For instance H-02-A, the algorithm terminated after the second iteration, since Gurobi did not accept the solution from iteration 2 as initial solution for the third ADM iteration and was not able to find another feasible solution within the limit of 2000 branch-and-bound nodes. Although this cannot happen in theory, it might happen in practice due to numerical issues, which are for instance due to scaling, aggregation or other MIP presolving algorithms. For all other instances, our ADM algorithm converged (to an infeasible point) within the iteration limit.

Since these results are not satisfactory, we slightly modify our algorithm by adding Constraint (23) to the set of constraints when Problem (31) is solved for calorific values. Although this modification is not in accordance with the theoretical framework presented in Section 3, we are able to obtain by far better results for both networks as can be seen in Table 3 and 4. Since Equation (23) is always satisfied in this case, we have $\Delta_{\text{mix}} = 0$ and we omit the corresponding column in Tables 3 and 4. The maximum number of ADM iterations has been set to 30.

TABLE 2. Results on the H-gas instances.

Instance	$\|\Delta_P\|_\infty$	$\|\Delta_P^{\mathrm{rel}}\|_\infty$	$\|\Delta_{\mathrm{mix}}\|_\infty$	$\|\Delta_\pi\|_\infty$	N	Time
H-01-A	3.40×10^2	0.1029	1.84×10^3	0.00	10	30003
H-01-B	1.59×10^1	0.1092	1.43×10^3	0.00	10	17485
H-01-C	1.59×10^1	0.1092	1.43×10^3	0.00	10	18496
H-02-A	4.02×10^1	0.1046	2.18×10^3	6.05	2	5466
H-02-B	8.41×10^1	0.1029	1.89×10^3	0.00	10	23971
H-02-C	1.72×10^2	0.1148	1.57×10^3	0.00	10	23978
H-03-A	5.23×10^1	0.1046	9.81×10^2	0.00	10	15067
H-03-B	1.62×10^2	0.1045	1.15×10^3	3.71	10	17912
H-03-C	1.62×10^2	0.1045	1.15×10^3	3.71	10	17925
H-04-A	4.43×10^2	0.1046	1.67×10^3	1.39	10	22959
H-04-B	4.37×10^2	0.1400	4.12×10^3	0.00	10	19290
H-04-C	5.72×10^2	0.1401	4.08×10^3	0.00	10	24034
H-05-A	4.43×10^2	0.1046	2.95×10^3	0.89	10	22915
H-05-B	4.37×10^2	0.1399	4.43×10^3	0.20	10	21065
H-05-C	5.75×10^2	0.1401	3.14×10^3	1.02	10	23930
H-06-A	2.96×10^2	0.1399	4.01×10^3	0.00	10	19177
H-06-B	4.46×10^2	0.1401	4.07×10^3	0.91	10	19924
H-06-C	6.42×10^2	0.1401	1.96×10^3	0.00	10	21900
H-07-A	1.62×10^2	0.1400	2.11×10^3	0.00	10	33213
H-07-B	1.08×10^2	0.1401	2.18×10^3	0.00	10	25555
H-07-C	8.12×10^1	0.1305	2.10×10^3	0.16	10	32533
H-08-A	2.12×10^2	0.1046	4.73×10^3	0.00	10	24999
H-08-B	9.96×10^1	0.1401	3.32×10^3	0.00	10	20287
H-08-C	1.92×10^2	0.1400	4.24×10^3	0.86	10	22730
H-09-A	3.44×10^2	0.1229	1.50×10^3	0.00	10	20419
H-09-B	5.65×10^2	0.1401	1.52×10^3	0.02	10	17939
H-09-C	1.26×10^2	0.1400	1.71×10^3	1.21	10	23498
H-10-A	2.12×10^2	0.1046	1.82×10^3	0.00	10	25263
H-10-B	2.56×10^2	0.1267	2.09×10^3	0.00	10	21040
H-10-C	2.20×10^2	0.1401	3.21×10^3	0.00	10	24634

For the L-gas network, the ADM algorithm finds a feasible solution to all instances. Most of the instances are solved within 3 or 4 ADM iterations. The maximum number of iterations is 6 for instance L-15. The average running time is 2020 s. The maximum running time of 4131 s has been needed to solve instance L-01. Since the running time for the solution of the LPs is negligible, the amount of time needed to solve the MIP models is virtually equal to the overall running time. The sizes of the MIP models do not vary significantly. For the L-gas network the MIP models consist of approximately 35 000 variables, whereof 8000 are binary, and 100 000 constraints.

For the H-gas network, three of the instances given in Table 4 could not be solved within the applied iteration limit. In all three cases, the value of $\|\Delta_\pi\|_\infty$ was still above the threshold of 0.1 bar in the end of iteration 30. Also instance H-08-C could not be solved, since we were not able to find an initial feasible solution in iteration 1. All other instances have been solved and for most of these only 10 iterations or less have been needed. As expected, the average runtime of 10 046 s is higher than for the L-gas network. Again the sizes of the MIP models do not vary significantly and

TABLE 3. Results on the L-gas instances for the modified ADM.

Instance	$\|\Delta_P\|_\infty$	$\|\Delta_P^{\text{rel}}\|_\infty$	$\|\Delta_\pi\|_\infty$	N	Time
L-01	4.21×10^{-1}	0.0257	0.00	4	4131
L-02	3.63×10^{-2}	0.0000	0.00	4	943
L-03	6.75×10^{-2}	0.0000	0.00	4	536
L-04	3.76×10^{-1}	0.0151	0.00	3	460
L-05	6.64×10^{-2}	0.0000	0.00	3	313
L-06	6.61×10^{-2}	0.0000	0.00	3	590
L-07	6.72×10^{-2}	0.0000	0.00	3	1089
L-08	2.34×10^{-1}	0.0029	0.00	4	2774
L-09	5.12×10^{-1}	0.0022	0.00	4	3968
L-10	2.58×10^{-1}	0.0095	0.00	4	1514
L-11	2.38×10^{-1}	0.0312	0.00	3	1152
L-12	4.53×10^{-2}	0.0000	0.00	4	2752
L-13	8.38×10^{-1}	0.0110	0.00	3	2637
L-14	1.83	0.0111	0.00	3	1617
L-15	1.81×10^{-2}	0.0000	0.00	6	2671
L-16	2.49×10^{-1}	0.0028	0.00	3	1647
L-17	5.52×10^{-1}	0.0110	0.00	3	1697
L-18	4.93×10^{-2}	0.0000	0.00	5	3940
L-19	1.82	0.0472	0.00	3	2148
L-20	2.74×10^{-1}	0.0124	0.00	3	2423
L-21	8.79×10^{-1}	0.0111	0.00	3	2569
L-22	7.78×10^{-1}	0.0111	0.00	3	2127
L-23	4.03×10^{-2}	0.0000	0.00	4	1762
L-24	2.55×10^{-1}	0.0113	0.00	3	2432
L-25	2.45×10^{-1}	0.0688	0.00	3	3090
L-26	2.71×10^{-2}	0.0000	0.00	5	1705
L-27	2.27×10^{-2}	0.0000	0.00	5	1175
L-28	4.45×10^{-1}	0.0096	0.00	3	1473
L-29	3.72×10^{-1}	0.0624	0.00	3	1741
L-30	4.68×10^{-2}	0.0000	0.00	4	2215
L-31	1.17×10^{-1}	0.0061	0.00	5	3857
L-32	2.97×10^{-2}	0.0000	0.00	4	1692
L-33	3.64×10^{-1}	0.0383	0.00	3	1805

are about 90 000 constraints and 72 000 variables, whereof approximately 12 000 are binary.

5. Conclusions

We presented a novel solution algorithm for nonconvex MINLPs arising in gas transport optimization. From an application point of view, the main contribution of the paper is the incorporation of heat power supply and demand as well as the required mixing model for different gas qualities. The resulting problem is a nonconvex MINLP containing nonsmooth pooling-like mixing equations. These problems were never solved before on real-world transport networks of the size like in this paper and thus, our results really mark a new milestone in solving large-scale nonconvex MINLPs on networks. From our point of view, the obtained computational results are based on two key ingredients. First, piecewise linear relaxation techniques allow to exploit the capability of today's MIP solvers for

TABLE 4. Results on the H-gas instances for the modified ADM.

Instance	$\|\Delta_P\|_\infty$	$\|\Delta_P^{\text{rel}}\|_\infty$	$\|\Delta_\pi\|_\infty$	N	Time
H-01-A	2.62×10^{-1}	0.0002	0.00	22	29550
H-01-B	6.20×10^{-1}	0.0058	0.00	11	12277
H-01-C	2.00×10^{-2}	0.0000	0.00	10	15964
H-02-A	3.26×10^{-2}	0.0000	0.00	5	2851
H-02-B	4.10×10^{-1}	0.0033	0.00	4	2994
H-02-C	1.38×10^{-1}	0.0039	0.00	8	7339
H-03-A	9.43	0.0034	0.00	5	4797
H-03-B	2.73×10^{-2}	0.0000	0.00	4	1055
H-03-C	2.73×10^{-2}	0.0000	0.00	4	1068
H-04-A	7.94	0.0396	0.00	20	6514
H-04-B	2.14×10^{-2}	0.0000	2.07	30	35722
H-04-C	3.65×10^{-2}	0.0000	0.00	8	5773
H-05-A	7.96	0.0396	0.00	7	4452
H-05-B	2.95×10^{-2}	0.0000	2.53	30	37322
H-05-C	2.20×10^{-2}	0.0000	0.00	5	5724
H-06-A	1.55×10^{-1}	0.0000	0.00	8	7484
H-06-B	8.88×10^{-2}	0.0000	0.00	8	8752
H-06-C	7.04×10^{-2}	0.0000	0.00	17	13954
H-07-A	2.24×10^{-1}	0.0084	0.00	4	4303
H-07-B	8.37×10^{-1}	0.0070	0.00	7	9682
H-07-C	3.36×10^{-1}	0.0103	0.00	6	4137
H-08-A	2.71×10^{-2}	0.0000	0.00	7	8720
H-08-B	2.77×10^{-2}	0.0000	0.00	8	9328
H-08-C	—	—	—	—	—
H-09-A	1.82×10^{-2}	0.0000	0.00	8	4813
H-09-B	1.93×10^{-2}	0.0000	0.13	30	18203
H-09-C	2.00×10^{-2}	0.0000	0.10	14	10144
H-10-A	2.33×10^{-2}	0.0000	0.00	6	4415
H-10-B	6.44×10^{-1}	0.0090	0.00	4	2083
H-10-C	1.91×10^{-2}	0.0000	0.00	11	11924

solving large-scale MINLPs. This approach was also applied to "standard" gas transport models (i.e., models using flow supply and demand) in the recent past and very encouraging results were reported. Second, we decomposed the full MINLP model in a way that allows us to use a tailored ADM: The first model solved in an ADM iteration corresponds to standard gas transport models; see [18, 27]. The second model is an easily solvable LP that adjusts gas quality parameters to the current flow-pressure situation.

Due to the quality of our computational results, the application of MIP-based ADMs seems to be suitable for other hard problems arising in gas transportation. Possible topics include more sophisticated models of compressor machines together with their associated drives or the incorporation of other gas parameters to improve the quality of the physics model; see, e.g., [18, 33, 32].

ACKNOWLEDGEMENT

We wish to thank all our collaborators from *ForNe – Research Cooperation Network Optimization* and especially our industry partner, the Open Grid Europe GmbH, for their support and the provision of the network data. This research has

been performed as part of the Energie Campus Nürnberg and supported by funding through the "Aufbruch Bayern (Bavaria on the move)" initiative of the state of Bavaria. Lars Schewe acknowledges funding through the DFG Transregio TRR 154, Subproject B7.

References

[1] D. P. Bertsekas and J. N. Tsitsiklis. *Parallel and Distributed Computation: Numerical Methods*. Upper Saddle River, NJ, USA: Prentice-Hall, Inc., 1989.

[2] S. Boyd, N. Parikh, E. Chu, B. Peleato, and J. Eckstein. "Distributed Optimization and Statistical Learning via the Alternating Direction Method of Multipliers." In: *Found. Trends Mach. Learn.* 3.1 (Jan. 2011), pp. 1–122. DOI: 10.1561/2200000016.

[3] F. H. Clarke. *Optimization and nonsmooth analysis*. 2nd ed. Vol. 5. Classics in Applied Mathematics. Society for Industrial and Applied Mathematics (SIAM), Philadelphia, PA, 1990, pp. xii+308. DOI: 10.1137/1.9781611971309.

[4] E. Danna, E. Rothberg, and C. L. Pape. "Exploring relaxation induced neighborhoods to improve MIP solutions." In: *Mathematical Programming, Series A* 102 (2005), pp. 71–90.

[5] P. Domschke, B. Geißler, O. Kolb, J. Lang, A. Martin, and A. Morsi. "Combination of Nonlinear and Linear Optimization of Transient Gas Networks." In: *INFORMS Journal on Computing* 23.4 (2011), pp. 605–617.

[6] M. Feistauer. *Mathematical Methods in Fluid Dynamics*. Vol. 67. Pitman Monographs and Surveys in Pure and Applied Mathematics Series. Harlow: Longman Scientific & Technical, 1993.

[7] E. J. Finnemore and J. E. Franzini. *Fluid Mechanics with Engineering Applications*. 10th. McGraw-Hill, 2002.

[8] A. Fügenschuh, B. Geißler, R. Gollmer, C. Hayn, R. Henrion, B. Hiller, J. Humpola, T. Koch, T. Lehmann, A. Martin, R. Mirkov, A. Morsi, J. Rövekamp, L. Schewe, M. Schmidt, R. Schultz, R. Schwarz, J. Schweiger, C. Stangl, M. C. Steinbach, and B. M. Willert. "Mathematical Optimization for Challenging Network Planning Problems in Unbundled Liberalized Gas Markets." In: *Energy Systems* 5.3 (2013), pp. 449–473.

[9] D. Gabay and B. Mercier. "A dual algorithm for the solution of nonlinear variational problems via finite element approximation." In: *Computers & Mathematics with Applications* 2.1 (1976), pp. 17–40. DOI: 10.1016/0898-1221(76)90003-1.

[10] B. Geißler, O. Kolb, J. Lang, G. Leugering, A. Martin, and A. Morsi. "Mixed Integer Linear Models for the Optimization of Dynamical Transport Networks." In: *Mathematical Methods of Operations Research* 73.3 (2011), pp. 339–362.

[11] B. Geißler. "Towards Globally Optimal Solutions for MINLPs by Discretization Techniques with Applications in Gas Network Optimization." PhD thesis. Friedrich-Alexander-Universität Erlangen-Nürnberg (FAU), 2011.

[12] B. Geißler, A. Morsi, and L. Schewe. "A New Algorithm for MINLP Applied to Gas Transport Energy Cost Minimization." In: *Facets of Combinatorial Optimization*. Ed. by M. Jünger and G. Reinelt. Berlin, Heidelberg: Springer, 2013, pp. 321–353. DOI: 10.1007/978-3-642-38189-8_14.

[13] B. Geißler, A. Martin, A. Morsi, and L. Schewe. "Using Piecewise Linear Functions for Solving MINLPs." In: *Mixed Integer Nonlinear Programming*. Ed. by J. Lee and S. Leyffer. Vol. 154. The IMA Volumes in Mathematics and its Applications. Springer New York, 2012, pp. 287–314. DOI: 10.1007/978-1-4614-1927-3_10.

[14] R. Glowinski and A. Marroco. "Sur l'approximation, par éléments finis d'ordre un, et la résolution, par pénalisation-dualité d'une classe de problèmes de Dirichlet non linéaires." In: *ESAIM: Mathematical Modelling and Numerical Analysis - Modélisation Mathématique et Analyse Numérique* 9.R2 (1975), pp. 41–76.

[15] J. Gorski, F. Pfeuffer, and K. Klamroth. "Biconvex sets and optimization with biconvex functions: a survey and extensions." In: *Math. Methods Oper. Res.* 66.3 (2007), pp. 373–407. DOI: 10.1007/s00186-007-0161-1.

[16] Z. Gu, E. Rothberg, and R. Bixby. *Gurobi Optimizer Reference Manual, Version 5.6*. Gurobi Optimization Inc. Houston, USA, 2013.

[17] M. Jünger and G. Reinelt, eds. *Facets of Combinatorial Optimization*. Berlin, Heidelberg: Springer, 2013. DOI: 10.1007/978-3-642-38189-8.

[18] T. Koch, B. Hiller, M. E. Pfetsch, and L. Schewe, eds. *Evaluating Gas Network Capacities*. SIAM-MOS series on Optimization. SIAM, Dec. 2014. x + 375. Forthcoming.

[19] C. L. Lawson. "Characteristic properties of the segmented rational minimax approximation problem." In: *Numerische Mathematik* 6 (1964), pp. 293–301.

[20] X. Li, E. Armagan, A. Tomasgard, and P. I. Barton. "Stochastic pooling problem for natural gas production network design and operation under uncertainty." In: *AIChE J.* 57.8 (2011), pp. 2120–2135. DOI: 10.1002/aic.12419.

[21] M. V. Lurie. *Modeling of Oil Product and Gas Pipeline Transportation*. Weinheim: Wiley-VCH, 2008.

[22] A. Morsi. "Solving MINLPs on Loosely-Coupled Networks with Applications in Water and Gas Network Optimization." PhD thesis. Friedrich-Alexander-Universität Erlangen-Nürnberg (FAU), 2013.

[23] J. Nikuradse. *Laws of Flow in Rough Pipes*. Vol. Technical Memorandum 1292. National Advisory Committee for Aeronautics Washington, 1950.

[24] J. Nocedal and S. J. Wright. *Numerical Optimization*. 2nd ed. Springer Series in Operations Research and Financial Engineering. New York: Springer Verlag, 2006. DOI: 10.1007/978-0-387-40065-5.

[25] J. Papay. "A termeléstechnológiai paraméterek változása a gáztelepek muvelése során." In: *OGIL Musz. Tud. Kozl.* (1968).

[26] T. Pavlidis and A. P. Maika. "Uniform piecewise polynomial approximation with variable joints." In: *Journal of Approximation Theory* 12.1 (1974), pp. 61–69.

[27] M. E. Pfetsch, A. Fügenschuh, B. Geißler, N. Geißler, R. Gollmer, B. Hiller, J. Humpola, T. Koch, T. Lehmann, A. Martin, A. Morsi, J. Rövekamp, L. Schewe, M. Schmidt, R. Schultz, R. Schwarz, J. Schweiger, C. Stangl, M. C. Steinbach, S. Vigerske, and B. M. Willert. "Validation of nominations in gas network optimization: models, methods, and solutions." In: *Optimization Methods and Software* 30.1 (2015), pp. 15–53. DOI: 10.1080/10556788.2014.888426.

[28] M. J. D. Powell. *Approximation Theory and Methods*. Cambridge University Press, 1981.

[29] E. Remez. "Sur le calcul effectif des polynomes d'approximation de Tschebyscheff." In: *C. R. Acad. Sci.* 199 (1934), pp. 337–340.

[30] J. Saleh, ed. *Fluid Flow Handbook*. McGraw-Hill Handbooks. New York: McGraw-Hill, 2002.

[31] M. Schmidt, M. C. Steinbach, and B. M. Willert. "A Primal Heuristic for Nonsmooth Mixed Integer Nonlinear Optimization." In: *Facets of Combinatorial Optimization*. Ed. by M. Jünger and G. Reinelt. Berlin, Heidelberg: Springer, 2013, pp. 295–320. DOI: 10.1007/978-3-642-38189-8_13.

[32] M. Schmidt, M. C. Steinbach, and B. M. Willert. "High detail stationary optimization models for gas networks." In: *Optimization and Engineering* (2014), pp. 1–34. DOI: 10.1007/s11081-014-9246-x.

[33] M. Schmidt, M. C. Steinbach, and B. M. Willert. *High Detail Stationary Optimization Models for Gas Networks: Validation and Results.* Tech. rep. Submitted. Friedrich-Alexander-Universität Erlangen-Nürnberg, Department Mathematik; Leibniz Universität Hannover, Institut für Angewandte Mathematik, 2014. URL: http://www.optimization-online.org/DB_HTML/2014/10/4602.html.

[34] A. Tomasgard, F. Rømo, M. Fodstad, and K. Midthun. "Optimization Models for the Natural Gas Value Chain." In: *Geometric Modelling, Numerical Simulation, and Optimization.* Ed. by G. Hasle, K.-A. Lie, and E. Quak. Springer Verlag, New York, 2007, pp. 521–558.

[35] N. Trefethen. *Approximation Theory and Approximation Practice.* SIAM, 2013.

[36] T. van der Hoeven. "Math in Gas and the Art of Linearization." PhD thesis. Rijksuniversiteit Groningen, 2004.

[37] R. E. Wendell and A. P. Hurter Jr. "Minimization of a non-separable objective function subject to disjoint constraints." In: *Operations Res.* 24.4 (1976), pp. 643–657. DOI: 10.1287/opre.24.4.643.

[38] J. F. Wilkinson, D. V. Holliday, E. H. Batey, and K. W. Hannah. *Transient Flow in Natural Gas Transmission Systems.* American Gas Association, New York, 1964.

[1]Björn Geissler, Antonio Morsi, Lars Schewe, Friedrich-Alexander-Universität Erlangen-Nürnberg (FAU), Discrete Optimization, Cauerstr. 11, 91058 Erlangen, Germany, [2]Martin Schmidt, (a) Friedrich-Alexander-Universität Erlangen-Nürnberg, Discrete Optimization, Cauerstr. 11, 91058 Erlangen, Germany; (b) Energie Campus Nürnberg, Fürther Str. 250, 90429 Nürnberg, Germany

E-mail address: [1]{antonio.morsi,lars.schewe,bjoern.geissler}@math.uni-erlangen.de

E-mail address: [2]mar.schmidt@fau.de